



A generalized Fourier transform and convolution on time scales [☆]

Robert J. Marks II ^a, Ian A. Gravagne ^a, John M. Davis ^{b,*}

^a Department of Electrical and Computer Engineering, Baylor University, Waco, TX 76798, USA

^b Department of Mathematics, Baylor University, Waco, TX 76798 USA

Received 19 September 2006

Available online 12 September 2007

Submitted by Steven G. Krantz

Abstract

In this paper, we develop some important Fourier analysis tools in the context of time scales. In particular, we present a generalized Fourier transform in this context as well as a critical inversion result. This leads directly to a convolution for signals on two (possibly distinct) time scales as well as several natural classes of time scales which arise in this setting: dilated, closed under addition, and additively idempotent. We explore the properties of these time scales and demonstrate the utility of these concepts in discrete convolution, Mellin convolution, and transformations of a random variable.

© 2007 Elsevier Inc. All rights reserved.

Keywords: Fourier analysis; Generalized Fourier transform; Hilger circle; Time scale; Convolution

1. Introduction

The theory of time scales springs from the 1988 doctoral dissertation of Stefan Hilger [9] that resulted in his seminal paper [7] in 1990. These works aimed to unify and generalize various mathematical concepts from the theories of discrete and continuous dynamical systems. Afterwards, the body of knowledge concerning time scales advanced fairly quickly, culminating in the excellent introductory text by Bohner and Peterson [3] and their more recent advanced monograph [2]. A succinct survey on time scales can be found in [1].

Here, we explore time scales as a unification theory under which continuous and discrete time signals and systems are subsumed. In particular, we

- (1) establish that the time scale Fourier transformation introduced by Hilger [10] reduces to a form closely resembling the conventional continuous and discrete time Fourier transforms,
- (2) provide a method for inverting the Fourier transform on a time scale, and
- (3) perform a convolutional filtering operation on a class of time scales said to be *additively idempotent*.

[☆] This work was supported by NSF Grant EHS#0410685. For other papers from the Baylor Time Scales Research Group, please see <http://www.timescales.org/>.

* Corresponding author.

E-mail addresses: robert_marks@baylor.edu (R.J. Marks II), ian_gravagne@baylor.edu (I.A. Gravagne), john_m_davis@baylor.edu (J.M. Davis).

The bulk of engineering systems theory to date rests on two time scales, \mathbb{R} and \mathbb{Z} corresponding, respectively, to continuous and discrete signals and systems. Frequency analysis in \mathbb{R} is handled by the continuous time Fourier transform and, for \mathbb{Z} , the discrete time Fourier transform. These are both special cases of the Fourier transform on a time scale presented here. In the case of convolution, a signal in \mathbb{R} convolved with an impulse response in \mathbb{R} produces a response in \mathbb{R} . The same is true for \mathbb{Z} . We will show there exist numerous other time scales with interesting properties for which this is also true. Examples are given for transformations on a random variable and Mellin convolution.

2. Background

In this section, we quickly review the salient points of the theory needed to make this paper reasonably self-contained, but our treatment is by no means exhaustive.

2.1. Relevant time scales

We will use some standard and nonstandard examples of time scales throughout this paper. We organize them here for convenient reference. See Fig. 1 and Table 1. (We use the same ordering below.)

- (a) \mathbb{R} consists of the entire real line.
- (b) $h\mathbb{Z} := \{\dots, -2h, -h, 0, h, 2h, \dots\}$ for $h > 0$.
- (c) $h\mathbb{Z}_n$ contains the origin and points separated by an interval h beginning at nh . The time scale shown here is \mathbb{Z}_3 .
- (d) \mathbb{L}_k , for a specified k , consists of all points $\{t_n: t_n = \log(k(n - 1) + 1), n \in \mathbb{N}\}$. For example, $\mathbb{L}_1 = \{\log(1), \log(2), \log(3), \dots\}$ is shown in Fig. 1. The log base is arbitrary but fixed.
- (e) \mathbb{P}_{ab} consists of a union of closed intervals of length a each separated by a distance of b .
- (f) $\mathbb{Q}_{ab} = \bigcup_{n \in \mathbb{N}} \{na \leq t \leq nb\} \cup \{0\}$. There will be a time η where all $t \geq \eta$ are in \mathbb{Q}_{ab} , i.e. \mathbb{Q}_{ab} becomes a continuous interval for $t \geq \eta$. This occurs when the intervals begin to overlap. The n th and the $(n + 1)$ st intervals overlap when $nb \geq (n + 1)a$ or $n > \frac{a}{b-a}$. Then

$$\eta = \left(1 + \left\lfloor \frac{a}{b-a} \right\rfloor\right)a, \tag{2.1}$$

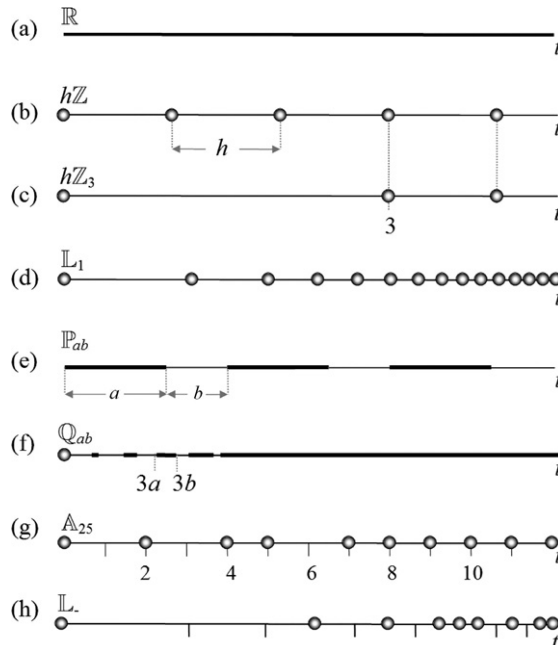


Fig. 1. Relevant time scales.

Table 1
Canonical time scales

$\mathbb{N} = \{1, 2, 3, \dots\}$	natural numbers
$\mathbb{R} = (-\infty, \infty)$	real numbers
$\mathbb{R}^+ = [0, \infty)$	nonnegative real numbers
\mathbb{T}	generic time scale
$h\mathbb{T} = \{ht: t \in \mathbb{T}\}$	uniform discrete time scale
$\mathbb{Z} = \{\dots, -3, -2, -1, 0, 1, 2, 3, \dots\}$	the integers
$\mathbb{Z}^+ = \{1, 2, 3, \dots\}$	the positive integers
$\mathbb{L}_k = \{\log(k(n-1) + 1): n \in \mathbb{N}\}$	log time scale
$\mathbb{D} = \{t_n\}$	(nonuniform) discrete time scale
\mathbb{X}	time scale on which $x(\tau)$ is defined
\mathbb{H}	time scale on which $h(\xi)$ is defined
\mathbb{Y}	time scale on which $y(t)$ is defined

where $\lfloor \psi \rfloor$ denotes the greatest integer not exceeding ψ . For example,

$$\mathbb{Q}_{10,13} = \{0\} \cup \{t: 10 \leq t \leq 13 \text{ or } 20 \leq t \leq 26 \text{ or } 30 \leq t \leq 39 \text{ or } t \geq 40\}.$$

Thus, as required by (2.1), $\eta = (1 + \lfloor \frac{10}{13-10} \rfloor) \times 10 = 40$.

(g) $\mathbb{A}_{\xi\eta} := \{0\} \cup \{n\xi + m\eta: n, m \in \mathbb{N}\}$. Shown in Fig. 1 is

$$\mathbb{A}_{2,5} = \{0, 2, 4, 5, 7, 8, 9, 10, 11, \dots\}.$$

(h) $\mathbb{L}_- := \mathbb{L}_1 \setminus \{\log p: p \text{ prime}\}$.

Definition 2.1. A causal time scale is a time scale that contains no values of t less than zero.

For example, \mathbb{R}^+ and \mathbb{Z}^+ are the causal time scales \mathbb{R} and \mathbb{Z} for $t \geq 0$. The time scales \mathbb{R} and \mathbb{R}^+ are the time scales used for continuous time signals and systems, while \mathbb{Z} and \mathbb{Z}^+ are the time scales of discrete time signals and systems. The time scales \mathbb{N} and \mathbb{L}_k are also causal.

2.2. The Hilger complex plane

Definition 2.2. For $h > 0$, define the Hilger complex numbers, the Hilger real axis, the Hilger alternating axis, and the Hilger imaginary circle by

$$\begin{aligned} \mathbb{C}_h &:= \left\{ z \in \mathbb{C}: z \neq -\frac{1}{h} \right\}, & \mathbb{R}_h &:= \left\{ z \in \mathbb{R}: z > -\frac{1}{h} \right\}, \\ \mathbb{A}_h &:= \left\{ z \in \mathbb{R}: z < -\frac{1}{h} \right\}, & \mathbb{I}_h &:= \left\{ z \in \mathbb{C}: \left| z + \frac{1}{h} \right| = \frac{1}{h} \right\}, \end{aligned}$$

respectively. For $h = 0$, let $\mathbb{C}_0 := \mathbb{C}$, $\mathbb{R}_0 := \mathbb{R}$, $\mathbb{A}_0 := \emptyset$, and $\mathbb{I}_0 := i\mathbb{R}$. See Fig. 2.

The Hilger complex plane, pictured on the left in Fig. 2, is akin to the s plane of the one-sided Laplace transforms and the z plane of the one-sided z transform. Stability is associated with the shaded interior of the Hilger circle [2]. The circle, centered at $-1/\mu(t)$, opens to the entire left plane as $\mu \rightarrow 0^+$, i.e. when the time scale becomes continuous. We are, in essence, in the s domain. When $\mu = 1$, the Hilger circle is the shifted unit circle in the z plane.¹

Definition 2.3. For $h > 0$, define the strip $\mathbb{Z}_h := \{z \in \mathbb{C}: -\frac{\pi}{h} < \text{Im}(z) \leq \frac{\pi}{h}\}$, and for $h = 0$, set $\mathbb{Z}_0 := \mathbb{C}$. Then we can define the cylinder transformation $\xi_h: \mathbb{C}_h \rightarrow \mathbb{Z}_h$ by

$$\xi_h(z) = \frac{1}{h} \text{Log}(1 + zh), \quad h > 0, \tag{2.2}$$

¹ The unit circle in the z plane is typically centered around the origin. The circle's shift comes from our consideration of equations of the form $x^\Delta(t) = px(t)$ rather than of the form of the equivalent difference type equation of the form $x(t + \mu(t)) = (\mu(t)p + 1)x(t)$.

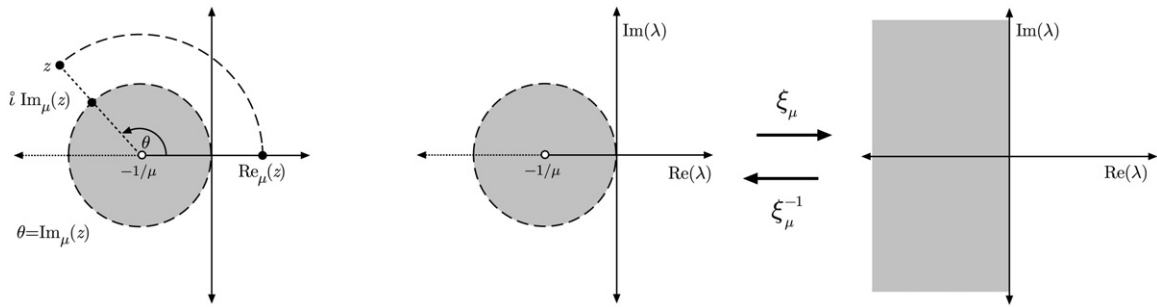


Fig. 2. (Left) The Hilger complex plane. (Right) The cylinder (2.2) and inverse cylinder (2.3) transformations map the familiar stability region in the continuous case to the interior of the Hilger circle in the general time scale case.

where Log is the principal logarithm function. When $h = 0$, we define $\xi_0(z) = z$, for all $z \in \mathbb{C}$. The cylinder transformation maps the interior of the Hilger circle to the left half plane.

The *inverse cylinder transformation* $\xi_h^{-1} : \mathbb{Z}_h \rightarrow \mathbb{C}_h$ is given by

$$\xi_h^{-1}(z) = \frac{e^{zh} - 1}{h}. \tag{2.3}$$

Definition 2.4. The Hilger pure imaginary number [2], around the periphery of the Hilger circle, is²

$$i 2\pi u = \xi_h^{-1}(j2\pi u) = \frac{e^{j2\pi u} - 1}{h},$$

where $j = \sqrt{-1}$. See Fig. 2.

Definition 2.5. The function $p : \mathbb{T} \rightarrow \mathbb{R}$ is *regressive* if $1 + \mu(t)p(t) \neq 0$ for all $t \in \mathbb{T}^\kappa$, and we denote

$$\mathcal{R} = \{p : \mathbb{T} \rightarrow \mathbb{R} : p \in C_{rd}(\mathbb{T}) \text{ and } 1 + \mu(t)p(t) \neq 0 \forall t \in \mathbb{T}^\kappa\}.$$

Definition 2.6. If $p \in \mathcal{R}$, then we define the *generalized time scale exponential function* by

$$e_p(t, s) = \exp\left(\int_s^t \xi_{\mu(\tau)}(p(\tau)) \Delta\tau\right), \quad \text{for all } s, t \in \mathbb{T}.$$

If $p \in \mathcal{R}$, $y(t) = e_p(t, t_0)$ is the unique solution to the first order equation $y^\Delta(t) = p(t)y(t)$, $t \in \mathbb{T}$. Finally, note that $e_{\ominus z}(t, s) = 1/e_z(t, s)$ where \ominus is the operation from [2].

3. The Fourier transform on a time scale

Hilger [10] defines the Fourier transform on a time scale \mathbb{T} as

$$X(u) := \int_{t \in \mathbb{T}} x(t) e_{\ominus i 2\pi u}(t, 0) \Delta t.$$

Evaluation of the kernel reduces this to a more familiar form:

$$e_{\ominus i 2\pi u}(t, 0) = 1/e_{\xi^{-1}(j2\pi u)}(t, 0) = \exp\left(-\int_0^t \xi(\xi^{-1}(j2\pi u)) \Delta t\right) = e^{-j2\pi ut}.$$

² We use $2\pi u$ in lieu of ω to maintain Fourier transform symmetry. See [11].

Thus, the Fourier transform on a time scale \mathbb{T} can be written [8]

$$X(u) = \mathcal{F}\{x\}(u) := \int_{t \in \mathbb{T}} x(t)e^{-j2\pi ut} \Delta t. \tag{3.1}$$

There is an important distinction between the approach we choose to take here with the generalized Fourier transform versus the ones in [2,4]. Unlike those papers, our goal is *not* the distillation of all transform tables on all time scales to a single one. Instead, we want a transform that will result in an algebraically useful convolution and one that arises naturally from the dilation of two time scales. However, there is still a unification theme present in (3.1): one *does* obtain the canonical discrete and continuous Fourier transforms simply by choosing $\mathbb{T} = \mathbb{Z}$ and $\mathbb{T} = \mathbb{R}$ (respectively) in our definition.

We present some examples to illustrate this concept. Throughout, we have use the notation $y^\mu(t) := y(t)\mu(t)$, for $\mu(t) > 0$.

Example 3.1. Although the support of a signal may prove useful in assessing a time scale, it is inappropriate to equate the support of a signal to a corresponding time scale. The Fourier transform of a signal, for example, is a function of the time scale. On \mathbb{R} , consider the function

$$x(t) = \begin{cases} 0, & t < 0, \\ 1, & t = 0, \\ 0, & 0 < t < 3, \\ e^{t-3}U(t-3), & t \geq 3. \end{cases}$$

Modeling this signal on the time scale $\mathbb{T} = \{0\} \cup [3, \infty)$ produces a Fourier transform in (3.1) of $X(u) = 3 + e^{-j6\pi u}(1 + j2\pi u)^{-1}$. For the time scale $\mathbb{T} = \{0, 1\} \cup [3, \infty)$, the Fourier transform is

$$X(u) = 1 + e^{-j6\pi u}(1 + j2\pi u)^{-1}.$$

Example 3.2. The choice of the time scale changes the interpretation of $x^\mu(t)$ and will generally alter its Fourier transform significantly. To illustrate, let $x^\mu(t) = e^{-\alpha t}$ with $\text{Re } \alpha > 1$. On the time scale \mathbb{Z}^+ , the Fourier transform is $X(u) = (1 - e^{\alpha + j2\pi u})^{-1}$. For the time scale $\mathbb{L}_1 = \{t_n: t_n = \log(n), n \in \mathbb{N}\}$, we see $X(u) = \sum_{n=1}^\infty e^{-t_n} e^{-j2\pi ut_n} = \zeta(\alpha + j2\pi u)$, where

$$\zeta(z) = \sum_{n=1}^\infty \frac{1}{n^z}, \quad \text{Re } z > 1,$$

is the Riemann zeta function.

Example 3.3. In \mathbb{R} and \mathbb{Z} , the Fourier transform of a sinusoid is a Dirac delta functional centered at the frequency of the sinusoid. If the sinusoid is of finite duration, the transform is a sharp peak centered at the sinusoid frequency. Consider \mathbb{L}_1 using base \log_{10} . Figure 3 shows the Fourier transform of the signal corresponding to $x^\mu(t) = \cos(2\pi ft)\Pi_{20,000}(t)$ for $f = 4$, where

$$\Pi_K(t) := \begin{cases} 1, & 1 \leq t_n \leq t_K, \\ 0, & \text{otherwise.} \end{cases}$$

Since $x^\mu(t)$ is a sinusoid with frequency $f = 4$, we expect the transform to peak at $u = f = 4$ as shown. An analogous example for $x(t) = \cos(2\pi ft)\Pi_{20,000}(t)$ is shown in Fig. 4. In both figures, the real and imaginary portions of $X(u)$ are shown in the bottom right and bottom left.

Example 3.4. Figure 5 shows the magnitudes of the time scale Fourier transform for $x(t) = \cos(2\pi ft)\Pi_K(t)$ for $f = 10$ on \mathbb{L}_1 for $K = \{100, 1000, 10000, 100000\}$. All plots are on the same scale. A similar figure for $x^\mu(t) = \cos(2\pi ft)\Pi_K(t)$ for $f = 10$ is shown in Fig. 6, but with a varying plot range.

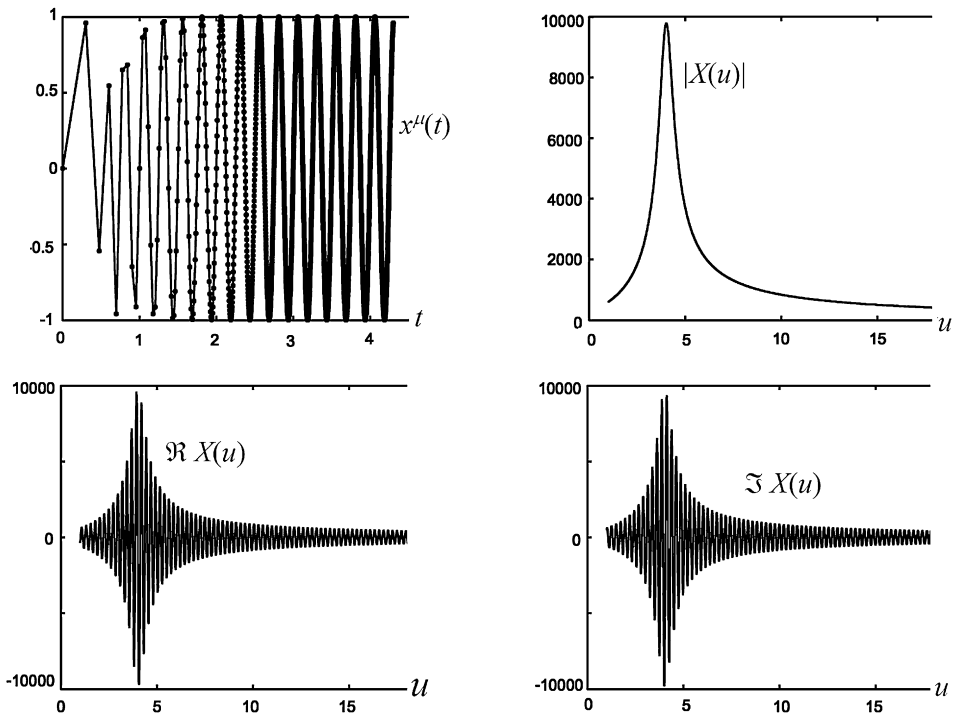


Fig. 3. (Top left) $x^\mu(t) = \cos(8\pi t)\Pi_{20,000}(t)$ on the time scale \mathbb{L}_1 . The dots denote the values of the function on the time scale and are linearly connected for clarity of presentation. (Top right) The magnitude of the time scale Fourier transform. (Bottom) The real and imaginary parts of the time scale Fourier transform.

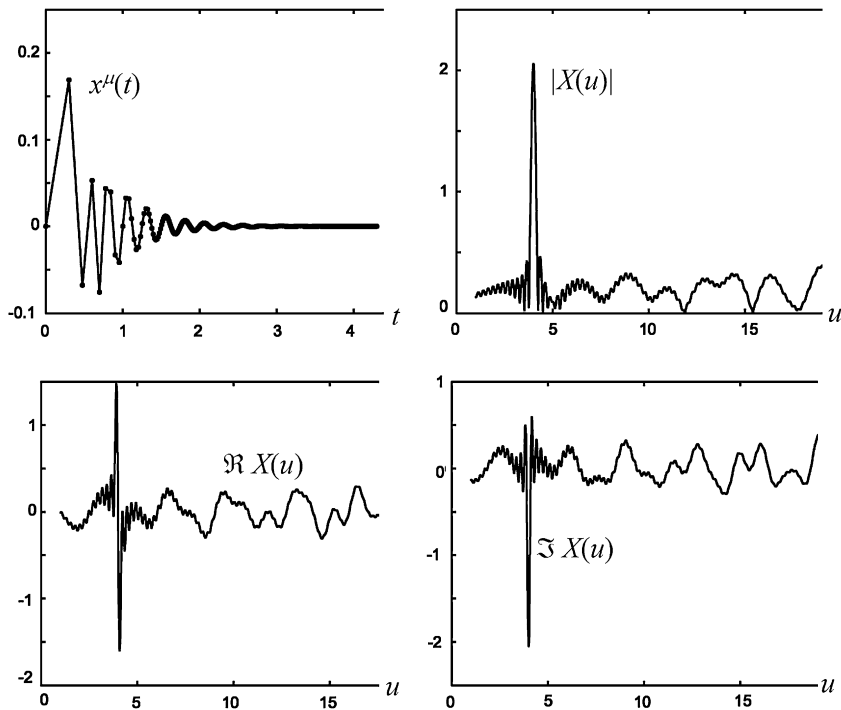


Fig. 4. These plots are the same as in Fig. 3, except the transform is of $x(t) = \cos(8\pi t)\Pi_{20,000}(t)$ rather than x^μ . The magnitude of the time scale Fourier transform, shown in the top right plot, peaks at the frequency $u = 4$.

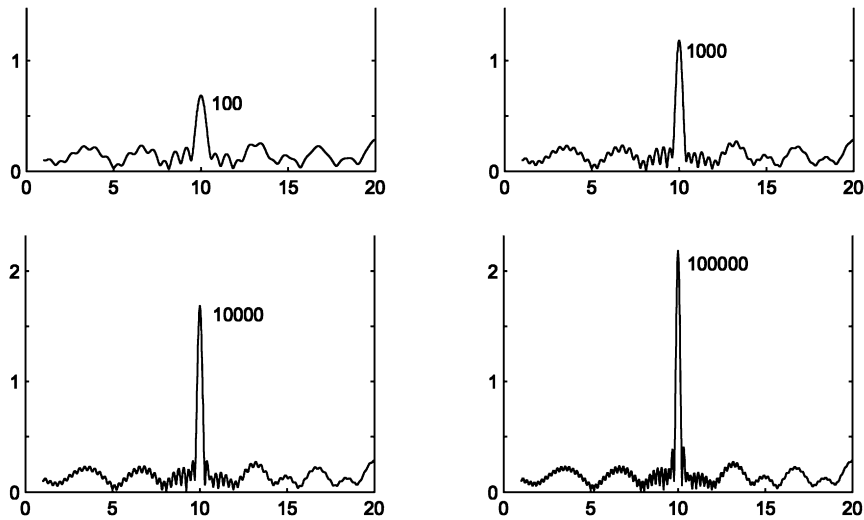


Fig. 5. The magnitudes of the time scale Fourier transform of a sinusoid $x(t) = \cos(2\pi ft)\Pi_K(t)$ with frequency $f = 10$ on \mathbb{L}_1 for various durations K . The longer the duration, the sharper the peak centered around $u = 10$. Fourier transforms on \mathbb{R} and \mathbb{Z} exhibit similar behavior.

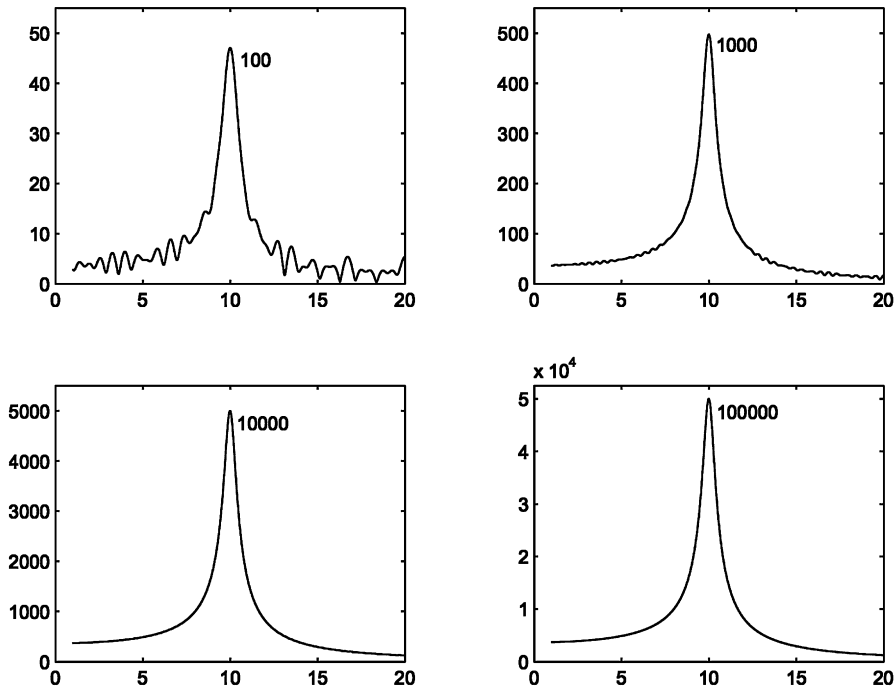


Fig. 6. Analogous to Fig. 5, except with $x^\mu(t) = \cos(2\pi ft)\Pi_K(t)$. As in Fig. 5, the longer the duration, the sharper the peak centered around $u = 10$.

Hilger [10] studied the time scale Fourier transform for $\mathbb{T} = \mathbb{R}$ and $\mathbb{T} = h\mathbb{Z}$. The purpose was to provide a seamless time scale theory for \mathbb{R} and $h\mathbb{Z}$ only. For $\mathbb{T} = h\mathbb{Z}$, inversion is obtained by integrating around the Hilger circle,

$$x(t) = \int_{-B}^B X(u)e^{j2\pi ut} du, \quad t \in h\mathbb{Z},$$

where $2B = \frac{1}{h}$. We note, however, that for $h\mathbb{Z}$, $X(u)$ is periodic and for this inversion the integration is over a single period.

Consider the more general case when the time scale is a set of discrete points in time but not necessarily equidistant, i.e. $\mathbb{T} = \mathbb{D} = \{t_n\}$. The time scale Fourier transform in (3.1) is no longer periodic if the t_n 's are not uniformly spaced. The Hilger circle, with radius $2B(t) = 1/\mu(t)$, now changes from point to point. Instead of integrating around the Hilger circle once, we will show that inverse Fourier transformation on an arbitrary time scale can be achieved by averaging repeated integrations.

Theorem 3.1 (Inversion of the time scale Fourier transform). *Let \mathbb{T} be a time scale and $X(u)$ be the Fourier transform of a signal on \mathbb{T} . Then $x(t)$ is given by*

$$x(t) = \mathcal{F}^{-1}\{X\}(t) := \lim_{N \rightarrow \infty} \frac{1}{2N+1} \sum_{n=-N}^N \int_{(2n-1)B(t)}^{(2n+1)B(t)} X(u) e^{j2\pi ut} du, \quad t \in \mathbb{T}. \tag{3.2}$$

Proof. First, suppose t is right-dense. Then $B(t) = \infty$ and (3.2) becomes the conventional continuous inverse Fourier transform:

$$\begin{aligned} \lim_{N \rightarrow \infty} \frac{1}{2N+1} \sum_{n=-N}^N \int_{(2n-1)B(t)}^{(2n+1)B(t)} X(u) e^{j2\pi ut} du &= \lim_{N \rightarrow \infty} \frac{1}{2N+1} \sum_{n=-N}^N \int_{-\infty}^{\infty} X(u) e^{j2\pi ut} du \\ &= \lim_{N \rightarrow \infty} \frac{1}{2N+1} \sum_{n=-N}^N x(t) \\ &= x(t). \end{aligned}$$

On the other hand, if t is right-scattered, then (3.2) becomes

$$\begin{aligned} \lim_{N \rightarrow \infty} \frac{1}{2N+1} \sum_{n=-N}^N \int_{(2n-1)B(t)}^{(2n+1)B(t)} X(u) e^{j2\pi ut} du &= \lim_{N \rightarrow \infty} \frac{1}{2N+1} \int_{-(2N+1)B(t)}^{(2N+1)B(t)} X(u) e^{j2\pi ut} du \\ &= \lim_{N \rightarrow \infty} \frac{1}{2N+1} \int_{-(2N+1)B(t)}^{(2N+1)B(t)} \left[\int_{\tau \in \mathbb{T}} x(\tau) e^{-j2\pi u\tau} \Delta\tau \right] e^{j2\pi ut} du \\ &= \int_{\tau \in \mathbb{T}} x(\tau) \left[\lim_{N \rightarrow \infty} \frac{1}{2N+1} \int_{-(2N+1)B(t)}^{(2N+1)B(t)} e^{j2\pi u(t-\tau)} du \right] \Delta\tau \\ &= \int_{\tau \in \mathbb{T}} x(\tau) \left[\lim_{N \rightarrow \infty} 2B(t) \operatorname{sinc}(2B(t)(2N+1)(t-\tau)) \right] \Delta\tau \\ &= 2B(t) \int_{\tau \in \mathbb{T}} x(\tau) \delta[t-\tau] \Delta\tau \\ &= x(t), \end{aligned}$$

where

$$\delta[w] := \begin{cases} 1, & w = 0, \\ 0, & w \neq 0, \end{cases} \quad \operatorname{sinc}(t) := \frac{\sin(\pi t)}{(\pi t)},$$

and we have used the property $\lim_{W \rightarrow \infty} \operatorname{sinc}(Wt) = \delta[t]$. \square

Theorem 3.1 requires *a priori* knowledge of the time scale. However, for discrete time scales, it is possible to invert Fourier transforms of signals on discrete time scales *without* such knowledge of the time scale. Except for points in \mathbb{D} where $x(t) = 0$, the time scale \mathbb{D} can be determined from $X(u)$.

Theorem 3.2. Let D be a discrete time scale and $X(u)$ be the time scale Fourier transform of a signal on D . Then

$$x^\mu(t) = \lim_{W \rightarrow \infty} \frac{1}{2W} \int_{-W}^W X(u) e^{j2\pi ut} du.$$

Proof. Substitute $W = B(t)(2N + 1)$ in the previous proof and let $W \rightarrow \infty$. \square

4. Convolution on time scales

The segue from a time scale Fourier transform to convolution on time scales is a natural one. Convolution of a signal in \mathbb{Z} with a signal in \mathbb{Z} results in a signal in \mathbb{Z} and convolution of a signal in \mathbb{R} with a signal in \mathbb{R} results in a signal in \mathbb{R} . For what other time scales does this property hold? In this section, we present such a class and outline various results.

Definition 4.1. The *dilation*³ [6] of two time scales \mathbb{X} and \mathbb{H} , denoted $\mathbb{X} \oplus \mathbb{H}$, is defined by

$$\mathbb{X} \oplus \mathbb{H} := \{x + h : x \in \mathbb{X}, h \in \mathbb{H}\}.$$

Example 4.1. Consider the following.

- (1) If $\mathbb{X} = \{0, 1\}$ and $\mathbb{H} = \{4, 5, 10\}$, then $\mathbb{X} \oplus \mathbb{H} = \{4, 5, 6, 10, 11\}$.
- (2) If $\mathbb{X} = \{0, 2\}$ and $\mathbb{H} = \{t : 0 \leq t \leq 1\}$, then $\mathbb{X} \oplus \mathbb{H} = \{t : 0 \leq t \leq 1 \text{ and } 2 \leq t \leq 3\}$.
- (3) If $\mathbb{X} = 2\mathbb{Z}$ and $\mathbb{H} = \mathbb{Z}$, then $\mathbb{X} \oplus \mathbb{H} = \mathbb{Z}$.
- (4) If $\mathbb{X} = \mathbb{L}_-$ and $\mathbb{H} = \mathbb{L}_1$, then $\mathbb{X} \oplus \mathbb{H} = \mathbb{L}_1$.

Time scale dilation is commutative and associative. The time scale containing only the origin, $\mathbb{I} = \{0\}$, is the identity element for dilation since for any \mathbb{T} , we have $\mathbb{T} \oplus \mathbb{I} = \mathbb{T}$. The time scale \mathbb{R} has the property that $\mathbb{T} \oplus \mathbb{R} = \mathbb{R}$ for all \mathbb{T} . Note that the dilation \oplus is not to be mistaken for \oplus from [2]. The context should make this clear.

Next, we propose a time scale convolution that results in the dilation of the component time scales. Our definition differs from that in Bohner and Peterson [2], but this is not surprising. The choice of a defining convolution is always dictated by the underlying transform. Bohner and Peterson’s convolution was developed in conjunction with the generalized Laplace transform which has a very different kernel than the generalized Fourier transform. Furthermore, we will see that several important properties follow from our definition.

Let $C \subset \mathbb{T}$ denote all points in \mathbb{T} that are right-dense and $D \subset \mathbb{T}$ be those that are not. Clearly $\mathbb{T} = C \cup D$. Then

$$\int_{t \in \mathbb{T}} y(t) \Delta t = \int_{-\infty}^{\infty} y_{\mathbb{R}}(t) dt,$$

where $y_{\mathbb{R}}(t) = y_C(t) \cup y_D(t)$,

$$y_D(t) = \sum_{\tau \in D} y^\mu(t) \delta(t - \tau),$$

where $\delta(t)$ denotes the Dirac delta, and

$$y_C(t) = \begin{cases} y(t), & t \in C, \\ 0, & t \notin C. \end{cases}$$

This enables us to define the following convolution product on the underlying dilated time scale.

³ Also called *Minkowski addition* in the literature [5].

Definition 4.2. Let $x : \mathbb{X} \rightarrow \mathbb{R}$ and $h : \mathbb{H} \rightarrow \mathbb{R}$. The convolution $x * h : \mathbb{Y} \rightarrow \mathbb{R}$ is given by

$$(x * h)(t) := \int_{\tau \in \mathbb{R}} x_{\mathbb{R}}(\tau) h_{\mathbb{R}}(t - \tau) d\tau,$$

where $\mathbb{Y} = \mathbb{X} \oplus \mathbb{H}$.

Theorem 4.1 (Convolution Theorem). Let $x(t) : \mathbb{X} \rightarrow \mathbb{R}$ have Fourier transform $X(u)$ and $h(t) : \mathbb{H} \rightarrow \mathbb{R}$ have Fourier transform $H(u)$, where \mathbb{X} and \mathbb{H} are time scales. Let $Y(u) := X(u)H(u)$ be the Fourier transform of $y(t)$. Then

$$\mathcal{F}\{y\} = \mathcal{F}\{x * h\} = X(u)H(u) = Y(u) = \int_{t \in \mathbb{Y}} y(t) e^{-j2\pi u t} \Delta t, \tag{4.1}$$

where $y(t)$ is defined on the dilated time scale $\mathbb{Y} = \mathbb{X} \oplus \mathbb{H}$.

Proof. Consider

$$\begin{aligned} Y(u) &= X(u)H(u) = \int_{\tau \in \mathbb{X}} x(\tau) e^{-j2\pi u \tau} \Delta \tau \int_{\xi \in \mathbb{H}} h(\xi) e^{-j2\pi u \xi} \Delta \xi \\ &= \int_{\tau \in \mathbb{R}} x_{\mathbb{R}}(\tau) e^{-j2\pi u \tau} d\tau \int_{\xi \in \mathbb{R}} h_{\mathbb{R}}(\xi) e^{-j2\pi u \xi} d\xi \\ &= \int_{\xi \in \mathbb{R}} \int_{\tau \in \mathbb{R}} x_{\mathbb{R}}(\tau) h_{\mathbb{R}}(\xi) e^{-j2\pi u(\tau + \xi)} d\tau d\xi \\ &= \int_{t \in \mathbb{R}} \left[\int_{\tau \in \mathbb{R}} x_{\mathbb{R}}(\tau) h_{\mathbb{R}}(t - \tau) d\tau \right] e^{-j2\pi u t} dt \\ &= \int_{t \in \mathbb{R}} y_{\mathbb{R}}(t) e^{-j2\pi u t} d\tau dt \\ &= \int_{t \in \mathbb{Y}} y(t) e^{-j2\pi u t} \Delta t \\ &= \mathcal{F}\{y\}, \end{aligned}$$

where

$$y_{\mathbb{R}}(t) = \int_{\tau \in \mathbb{R}} x_{\mathbb{R}}(\tau) h_{\mathbb{R}}(t - \tau) d\tau,$$

and $t = \tau + \xi$. For every $\tau \in \mathbb{X}$ and $\xi \in \mathbb{H}$, there is a $t = \tau + \xi \in \mathbb{Y} = \mathbb{X} \oplus \mathbb{H}$. \square

Since $y_{\mathbb{R}}(t) = 0$ for $t \notin \mathbb{Y}$, a corresponding signal $y(t)$ on a time scale \mathbb{Y} can be constructed to satisfy (4.1). The function $y(t)$, however, can contain Dirac deltas at right dense locations even if neither $x(t)$ or $h(t)$ contains Dirac deltas at right dense locations, e.g. there is a Dirac delta at the right dense location $t = 10$ in Fig. 7.

Corollary 4.1 (Convolution on discrete time scales). Let \mathbb{X}, \mathbb{H} be discrete time scales, and $x : \mathbb{X} \rightarrow \mathbb{R}, h : \mathbb{H} \rightarrow \mathbb{R}$. Then the convolution product is given by

$$y^\mu(t_p) = \sum_S x^\mu(\tau_n) h^\mu(t_p - \tau_n), \tag{4.2}$$

where $t_p \in \mathbb{Y} = \mathbb{X} \oplus \mathbb{H}, \tau_n \in \mathbb{X}$, and $S := \{\tau_n \in \mathbb{X}: (t_p - \tau_n) \in \mathbb{H}\}$.

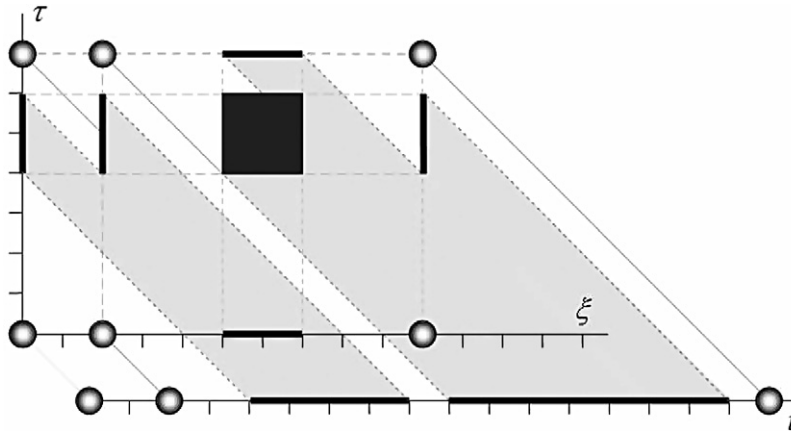


Fig. 7. Geometric interpretation of the dilation operation. The time scale $\mathbb{X} = \{\tau\} = \{0\} \cup [4, 5] \cup \{6\}$ and the time scale $\mathbb{H} = \{\xi\} = \{0\} \cup \{2\} \cup [5, 7] \cup \{10\}$. We take the Cartesian product of the time scales on the (ξ, τ) plane as shown. This Cartesian product, when multiplied by $e^{-j2\pi u t}$ and integrated, yields the Fourier transform, $Y(u)$. The family of lines corresponding to $t = \tau + \xi$ are shown. The shadow of the Cartesian product along these 45° lines contains the set of all $t = \tau + \xi$. This is the time scale $\mathbb{Y} = \mathbb{X} \oplus \mathbb{H} = \{t\} = \{0, 2\} \cup [4, 8] \cup [9, 16] \cup \{17\}$.

Proof. Again, consider

$$\begin{aligned} Y(u) &= X(u)H(u) = \sum_{\tau_n \in \mathbb{X}} x^\mu(\tau_n) e^{-j2\pi u \tau_n} \sum_{\xi_m \in \mathbb{H}} h^\mu(\xi_m) e^{-j2\pi u \xi_m} \\ &= \sum_{\xi_m \in \mathbb{H}} \sum_{\tau_n \in \mathbb{X}} x^\mu(\tau_n) h^\mu(\xi_m) e^{-j2\pi u (\xi_m + \tau_n)}. \end{aligned}$$

Now make the substitution $t_p = \tau_n + \xi_m$. Clearly, $t_p \in \mathbb{X} \oplus \mathbb{H} = \mathbb{Y}$. Then

$$Y(u) = \sum_{t_p \in \mathbb{Y}} \left[\sum_S x^\mu(\tau_n) h^\mu(t_p - \tau_n) \right] e^{-j2\pi u t_p}.$$

Since

$$Y(u) = \sum_{t_p \in \mathbb{Y}} y^\mu(t_p) e^{-j2\pi u t_p},$$

(4.2) follows immediately. \square

5. Classes of time scales arising from convolution

5.1. Dilated and closed under addition

In developing the time scale convolution, the dilation of two time scales arises naturally. We now investigate further consequences of the \oplus operation.

Definition 5.1. A time scale \mathbb{T} is *closed under addition*, if for every $\xi \in \mathbb{T}$ and $\tau \in \mathbb{T}$, the time $t = \xi + \tau \in \mathbb{T}$, i.e. $\mathbb{T} \oplus \mathbb{T} \subset \mathbb{T}$.

The time scales $h\mathbb{Z}$, $h\mathbb{Z}^+$, \mathbb{R} , \mathbb{R}_+ , $h\mathbb{Z}_n$, \mathbb{L}_k , \mathbb{Q}_{ab} , \mathbb{N} , and $\mathbb{A}_{\xi\eta}$ are closed under addition.

Example 5.1. Consider the following.

- (1) If $\mathbb{T} = \{-1, 0, 1\}$, then $\mathbb{T}_C = \mathbb{Z}$.
- (2) if $\mathbb{T} = \{t: 0 \leq t \leq 1\}$, then $\mathbb{T}_C = \mathbb{R}^+$.
- (3) if $\mathbb{T} = \{\frac{4}{5}, 1\}$, then $\mathbb{T}_C = \{\frac{4}{5}, 1, \frac{8}{5}, \frac{9}{5}, 2, \frac{12}{5}, \frac{13}{5}, \frac{14}{5}, 3, \frac{16}{5}, \frac{17}{5}, \frac{18}{5}, \frac{19}{5}, 4, \dots\}$.

A geometric interpretation of the dilation of two time scales is shown in Fig. 7. Here, \mathbb{X} is on the τ axis and \mathbb{H} is on the ξ axis. The Cartesian product of these time scales shows all allowable combinations of (ξ, τ) . All allowable points $t = \xi + \tau$ are shown as the shadow of the Cartesian product at 45° as shown. If a point t lies in the shadow of the Cartesian product, then there exists a (ξ, τ) such that $t = \xi + \tau$.

5.2. Additively idempotent time scales

If we strengthen the containment criterion in the definition of a time scale closed under addition, we introduce a class of time scales with a rich structure.

Definition 5.2. \mathbb{T} is *additively idempotent* (with respect to \oplus) if $\mathbb{T} \oplus \mathbb{T} = \mathbb{T}$.

We adopt the acronym AITS for *additively idempotent time scale*. Examples of AITS include $\mathbb{Z}, \mathbb{Z}^+, \mathbb{R}, \mathbb{R}^+, \mathbb{Z}_n, \mathbb{Q}_{ab}, \mathbb{A}_{\xi\eta}, \mathbb{L}_k$, and \mathbb{L}_- . \mathbb{N} is closed under addition but is not AITS. We now outline various properties and criteria for \mathbb{T} to be AITS.

Theorem 5.1 (*Characterization of AITS*).

- (a) A causal AITS must contain the origin.
- (b) If \mathbb{T} is closed under addition and contains the origin, then \mathbb{T} is AITS.
- (c) If \mathbb{T} is AITS, then $h\mathbb{T}$ is AITS.
- (d) All AITS other than \mathbb{I} are unbounded.
- (e) If \mathbb{T}_1 and \mathbb{T}_2 are both AITS, then $\mathbb{T}_3 = \mathbb{T}_1 \oplus \mathbb{T}_2$ is AITS.

Proof. (a) For $\mathbb{T} \in \mathbb{R}^+$: Let $\tau_0 = \inf\{t_n \in \mathbb{T}\}$. If $t_0 > 0$, then $t_0 \notin \mathbb{T} \oplus \mathbb{T}$, a contradiction.

(b) Since \mathbb{T} is closed under addition, $(\mathbb{T} \oplus \mathbb{T}) \subset \mathbb{T}$. Since $\mathbb{I} \subset \mathbb{T}$, we know $\mathbb{I} \oplus \mathbb{T} = \mathbb{T} \subset (\mathbb{T} \oplus \mathbb{T})$. Therefore $\mathbb{T} = \mathbb{T} \oplus \mathbb{T}$.

(c) $h\mathbb{T} \oplus h\mathbb{T} = \{h\alpha + h\beta: \alpha, \beta \in \mathbb{T}\} = h\{\alpha + \beta: \alpha, \beta \in \mathbb{T}\} = h\mathbb{T}$.

(d) Without loss of generality, consider the case when $t > 0$. Let $a \in \mathbb{T}$ and $a > 0$. Since \mathbb{T} is an AITS, $na \in \mathbb{T}$ and $na \rightarrow \infty$ as $n \rightarrow \infty$.

(e) $\mathbb{T}_3 \oplus \mathbb{T}_3 = (\mathbb{T}_1 \oplus \mathbb{T}_2) \oplus (\mathbb{T}_1 \oplus \mathbb{T}_2) = (\mathbb{T}_1 \oplus \mathbb{T}_1) \oplus (\mathbb{T}_2 \oplus \mathbb{T}_2) = \mathbb{T}_1 \oplus \mathbb{T}_2 = \mathbb{T}_3$. \square

Definition 5.3. Let \mathbb{T} be given. The AITS *hull* of \mathbb{T} , is the smallest (in the sense of inclusion) AITS, $\mathbb{T}_{\mathcal{A}}$, such that $\mathbb{T} \subset \mathbb{T}_{\mathcal{A}}$.

An AITS is illustrated in Fig. 8. The time scales for τ, ξ , and t are identical.

Example 5.2. We illustrate several of these concepts with the following examples:

- (1) $\mathbb{N} \oplus \mathbb{N} = \{2, 3, 4, \dots\} \subset \mathbb{N}$ and hence is closed under addition but, since $\mathbb{N} \oplus \mathbb{N} \neq \mathbb{N}$, we see that \mathbb{N} is not AITS.
- (2) $\mathbb{I}, \mathbb{R}, \mathbb{R}^+, h\mathbb{Z}$ and $h\mathbb{Z}^+$ are AITS.
- (3) The log time scale \mathbb{L}_k where $k \in \mathbb{N}$ is arbitrary but fixed, is AITS.
- (4) The time scale $\mathbb{L}_- = \{t_n = \log(n): n \text{ is composite}\}$ is AITS. This follows from the observation that since $\{0\} \in \mathbb{L}_-$, we know $\mathbb{L}_- \oplus \mathbb{L}_-$ contains \mathbb{L}_- . No logs of primes are in $\mathbb{L}_- \oplus \mathbb{L}_-$ because $t_n + t_m = \log(nm)$ and nm cannot be prime.
- (5) Assuming Goldbach’s conjecture, the closure of the set of $\{0\}$ and the set of all prime numbers is the AITS $\mathbb{Z}_2 = \{t: t = 0, n \geq 2\}$. To see this, note that Goldbach’s conjecture states that all even numbers exceeding two can be expressed as the sum of two prime numbers. Thus, all even integers greater than three are in $\mathbb{T}_{\mathcal{A}}$. Since they are prime, the numbers 2 and 3 are also in $\mathbb{T}_{\mathcal{A}}$. All odd numbers, $o > 5$, are in $\mathbb{T}_{\mathcal{A}}$ as the sum of three and the even number $o - 3$. More generally, $\mathbb{Z}_N = \{n \in \mathbb{Z}: n \geq N\} \cup \{0\}$ is an AITS.

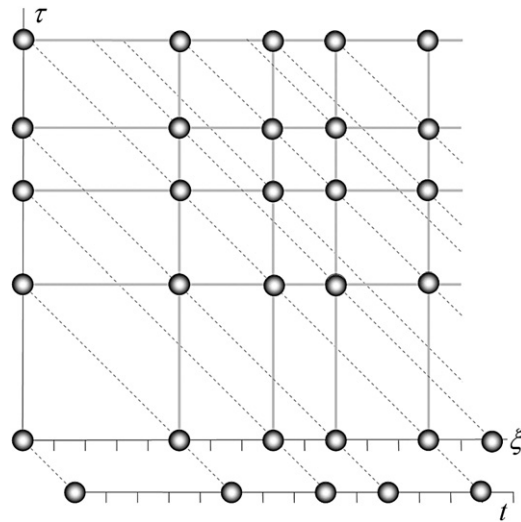


Fig. 8. Example of a discrete AITS. The time scales $\mathbb{X} = \mathbb{D}$ and $\mathbb{H} = \mathbb{D}$ on τ and ξ are identical. The 45° lines through all rectangular grid of points on the (ξ, τ) plane pass through points in \mathbb{D} on both the ξ and τ axes. The time scale \mathbb{D} is thus an AITS. The points generated by the 45° lines form, on the t axis, the same time scale $\mathbb{D} = \mathbb{D} \oplus \mathbb{D}$.

(6) (Piecewise accelerating time scales.) Consider the causal AITS $\mathbb{Z}_{10,5}^+ = \{0, 10, 20, 30, 35, 40, 45, 50, \dots\}$. This time scale is $10\mathbb{Z}$ until $t = 30$ and then becomes $5\mathbb{Z}$. In general, let N be expressed as the product of M integers $N = n_1 n_2 n_3 \dots n_M$. Then the following piecewise constant causal time scale is AITS:

$$\mathbb{Z}_{n_1, n_2, \dots, n_M}^+ = \begin{cases} N\mathbb{Z}^+, & 0 \leq t < p_1, \\ \frac{N}{n_1}\mathbb{Z}^+, & p_1 \leq t < p_2, \\ \frac{N}{n_1 n_2}\mathbb{Z}^+, & p_2 \leq t < p_3, \\ \frac{N}{n_1 n_2 n_3}\mathbb{Z}^+, & p_3 \leq t < p_4, \\ \vdots & \vdots \\ n_{M-1} n_M \mathbb{Z}^+, & p_{M-2} \leq t < p_{M-1}, \\ n_M \mathbb{Z}^+, & t \geq p_{M-1}, \end{cases}$$

where $0 < p_1 < p_2 < \dots < p_{M-1} < p_M$.

This relation extends to any AITS contained in \mathbb{R}^+ . If $\mathbb{T} \in \mathbb{R}^+$ is AITS, then

$$\mathbb{T}_{n_1, n_2, \dots, n_M} = \begin{cases} N\mathbb{T}, & 0 \leq t < p_1, \\ \frac{N}{n_1}\mathbb{T}, & p_1 \leq t < p_2, \\ \frac{N}{n_1 n_2}\mathbb{T}, & p_2 \leq t < p_3, \\ \frac{N}{n_1 n_2 n_3}\mathbb{T}, & p_3 \leq t < p_4, \\ \vdots & \vdots \\ n_{M-1} n_M \mathbb{T}, & p_{M-2} \leq t < p_{M-1}, \\ n_M \mathbb{T}, & p_{M-1} \leq t < p_M, \\ \mathbb{R}, & t \geq p_M, \end{cases}$$

is also AITS. Note we have allowed the time scale to become \mathbb{R} for $t \geq p_M$. This can be omitted by setting $p_m = \infty$.

(7) The AITS hull of $\{0, 7, 11\}$ is

$$\mathbb{A}_{7,11} = \{0, 7, 11, 14, 18, 21, 22, 25, 28, 29, 32, 33, 35, \dots\}.$$

More generally, the AITS hull of $\mathbb{T} = \{0, \xi, \eta\}$ is $\mathbb{T}_{\mathcal{A}} = \mathbb{A}_{\xi\eta}$.

(8) An AITS can be a mixed time scale containing both right-dense and right-scattered points. An example is the AITS hull of $\mathbb{T} = \{0\} \cup [a, b]$ where $0 < a < b$, which is $\mathbb{T}_{\mathcal{A}} = \mathbb{Q}_{ab}$. It is interesting to note that the Fourier transform of a signal, $x(t)$, on the time scale \mathbb{Q}_{ab} is

$$X(u) = \sum_{n=0}^{M-1} x^\mu(nb)e^{-j2\pi nbu} + \left[\sum_{n=1}^{M-1} \int_{t=na}^{nb} + \int_{t=Ma}^{\infty} \right] x(t)e^{-j2\pi ut} dt$$

where $M = \lfloor \frac{a}{b-a} \rfloor$.

The asymptotic graininess of an AITS can be described under certain conditions.

Theorem 5.2 (Asymptotic graininess for the hull of two relatively prime numbers). *Let $L, K \in \mathbb{N}$ be relatively prime and $K < L$. Define the time scale hull of $K\mathbb{T} = \{0, K, L\}$ as $K\mathbb{T}_{AITS}$. Then $K\mathbb{T}_{AITS}$ achieves a graininess of 1 at or before time $t = LK$ and maintains that constant graininess thereafter.*

Proof. When a graininess of one is achieved for K sequential integer times, say $\{p, p + 1, \dots, p + K - 1\}$, the graininess will be one thereafter. Since K is in the time scale, we assure unit graininess for the next K values by adding to the sequential integers to form $\{p + K, p + K + 1, \dots, p + 2K - 1\}$. Continuing this, we are assured that unit graininess occurs at time p and thereafter.

The proof is a straightforward result from residue number theory [14]. The time scale $K\mathbb{T}_{AITS}$ contains all integer multiples of K and L . These numbers, $\{\ell K : 1 \leq \ell \leq L\}$ and $\{kL : 1 \leq k \leq K\}$, form an additive basis from which all of the integers on $(KL, 2KL)$ can be formed. We require only K sequential integers to assure henceforth a graininess of one. This is guaranteed to occur, at least, for $\{KL, KL + 1, KL + 2, \dots, KL + (K - 1)\}$. Thus, the asymptotic graininess of one is achieved at least at time KL .

To see this, first denote $((n))_m$ as $n \bmod m$. Since L and K are relatively prime, the residues

$$((\ell K))_L, \quad 1 \leq \ell \leq L, \tag{5.1}$$

when arranged by magnitude, are $0, 1, 2, \dots, L - 1$. This follows from the fact that there are L residues in (5.1) and the following uniqueness argument: if $1 \leq \ell_1 \leq L$ and $1 \leq \ell_2 \leq L$ are such that $((\ell_1 K))_L = ((\ell_2 K))_L = r$, then $\ell_1 K = Lq_1 + r$ and $\ell_2 K = Lq_2 + r$. This forces $\ell_1 K - Lq_1 = \ell_2 K - Lq_2$ and hence $(\ell_1 - \ell_2)K = (q_1 - q_2)L$. But $\ell_1 = \ell_2$ if and only if $q_1 = q_2$. Similarly, the residues

$$((kL))_K, \quad 1 \leq k \leq K, \tag{5.2}$$

when arranged by magnitude, are $0, 1, 2, \dots, K - 1$. All of the residues correspond to different numbers on $1 \leq n \leq KL$ except the last: $((KL))_K = ((KL))_L = 0$.

Consider the numbers $KL < m < 2KL$. We find $((m))_L = \lambda$ and $((m))_K = \kappa$. There is a unique ℓ in the interval $1 \leq \ell \leq L$ such that $((\ell K))_L = \lambda$ and a unique k in the interval $1 \leq k \leq K$ such that $((kL))_K = \kappa$. Residue arithmetic then states $m = kL + \ell K$. Thus, since $kL \in K\mathbb{T}_{AITS}$ and $\ell K \in K\mathbb{T}_{AITS}$, all m in the interval $KL < m < 2KL$ are in $K\mathbb{T}_{AITS}$. In order to establish arrival at the asymptotic graininess of one, only K of these sequential values is needed. Thus, a graininess of one is achieved at $t = NL$ and remains thus thereafter. \square

To illustrate, let $K = 4$ and $L = 7$. Then (5.1) and (5.2) are

$$\begin{aligned} ((4))_7 = 4, \quad ((2 \times 4))_7 = 1, \quad ((3 \times 4))_7 = 5, \quad ((4 \times 4))_7 = 2, \quad ((5 \times 4))_7 = 6, \quad ((6 \times 4))_7 = 3, \\ ((7 \times 4))_7 = 0, \quad ((7))_4 = 3, \quad ((2 \times 7))_4 = 2, \quad ((3 \times 7))_4 = 1, \quad ((4 \times 7))_4 = 0, \end{aligned}$$

or

$$\begin{aligned} ((4))_7 = 4, \quad ((8))_7 = 1, \quad ((12))_7 = 5, \quad ((16))_7 = 2, \quad ((20))_7 = 6, \quad ((24))_7 = 3, \quad ((28))_7 = 0, \\ ((7))_4 = 3, \quad ((14))_4 = 2, \quad ((21))_4 = 1, \quad ((28))_4 = 0. \end{aligned} \tag{5.3}$$

The top mod 7 row contains the residues 0 through 6. The bottom contains the residues 0 through 3. The numbers represented on the top row are $\{4, 8, 12, 16, 20, 24, 28\}$ and, on the bottom, $\{7, 14, 21, 28\}$. Except for $KL = 28$, the numbers are distinct.

Consider $m = 33$. Clearly, $((33))_7 = 5$ and $((33))_4 = 1$. Since, from (5.3), $((12))_7 = 5$ and $((21))_4 = 1$, we obtain $12 + 21 = 33$, the desired answer.

The time scale for this example is

$$K\mathbb{T}_{\text{AITS}} = \{0, 4, 7, 8, 11, 12, 14, 15, 16, 18, 19, 20, 21, 22, 23, 24, 25, 26, 27, 28, \dots\}.$$

The theorem states unit graininess will begin no later than $t = LK = 28$. It clearly begins earlier at $t = 18$.

Theorem 5.3 (Asymptotic graininess for rational time scales). *The AITS hull of $\mathbb{T} = \{0, 1, \frac{L}{K}\}$ where $L, K \in \mathbb{N}$ are relatively prime and $L > K$ achieves additively idempotent hull of \mathbb{T}_{AITS} with asymptotic graininess $\mu = \frac{1}{K}$. Furthermore, this graininess is achieved at or before the time*

$$t_\mu = L + \frac{1}{L}(L - 1). \tag{5.4}$$

Proof. Since \mathbb{T} is a scaled version of $k\mathbb{T}$, the theorem follows immediately from Theorem 5.1(c). \square

On the other hand, we can handle the nonrelatively prime case as follows.

Lemma 5.1. *If \hat{K} and \hat{L} are not relatively prime, then the AITS hull of $\{0, \hat{K}, \hat{L}\}$ has an asymptotic graininess of G where G is the greatest common factor of \hat{K} and \hat{L} .*

Proof. Since $\{0, K, L\}$ has a hull with asymptotic graininess of one, $\{0, \hat{K}, \hat{L}\} = G\{0, K, L\}$ has a hull with an asymptotic graininess of G . \square

Lemma 5.2. *Let $\mathbb{T} = \{0, 1, x\}$ where x is irrational. Then the asymptotic graininess of \mathbb{T}_{AITS} is zero.*

Proof. As x is approximated more and more closely by the rational $p/10^q$ with $p, 10^q$ relatively prime, then $q \rightarrow \infty$ and $\mu \rightarrow 0$ by the previous theorem. Moreover, the time that this is achieved is $t_\mu = \infty$ by (5.4). \square

The previous lemmas yield the proof for the following result.

Theorem 5.4 (Asymptotic graininess of AITS hull). *All time scales hulls of the points $\{0, a, b\}$ where $0 < a < b$ form a causal time scale with constant asymptotic graininess.*

6. Examples of discrete convolution on AITS

Let \mathbb{D} be a discrete AITS, $x : \mathbb{D} \rightarrow \mathbb{R}$, and $h : \mathbb{D} \rightarrow \mathbb{R}$. Then y , the inverse Fourier transform of $Y(u) = X(u)H(u)$, also has time scale \mathbb{D} . The time scale convolution in (4.2) becomes

$$y^\mu(t_p) = \sum_{t_p - \tau_n \in \mathbb{D}} x^\mu(\tau_n)h^\mu(t_p - \tau_n), \quad t_p \in \mathbb{D}, \tag{6.1}$$

which we will write as

$$y^\mu(t) = x^\mu(t) \overset{\mathbb{D}}{*} h^\mu(t). \tag{6.2}$$

We now outline some examples of AITS convolution.

6.1. \mathbb{L}_1 convolution

For \mathbb{L}_1 , the time scale convolution in (6.1) is

$$y^\mu(t_p) = \sum_{p/n \in \mathbb{N}} x^\mu(t_n)h^\mu(t_p/n) \tag{6.3}$$

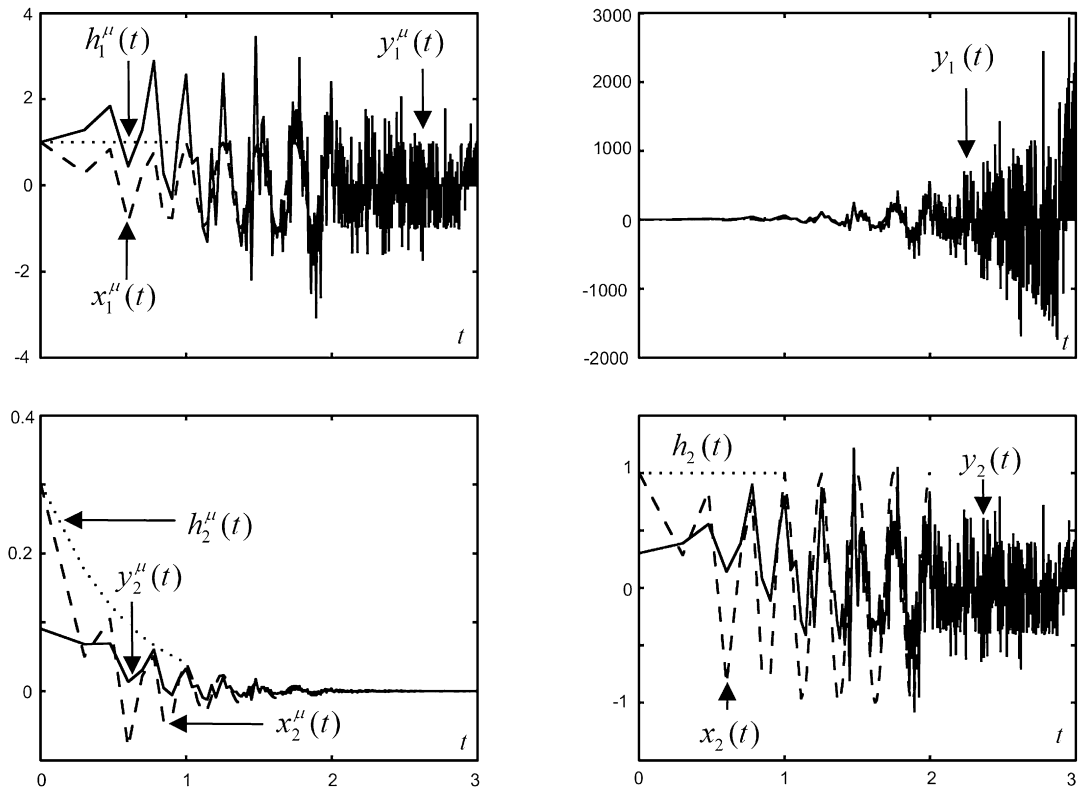


Fig. 9. The top left plot illustrates the time scale convolution on the time scale \mathbb{L}_1 of $x_1^\mu(t) = \cos(8\pi t)\Pi_{100}(t)$, shown with the dashed line, with $h_1^\mu(t) = \Pi_{10}(t)$ shown with the dotted line. Both functions are on the time scale \mathbb{L}_1 . The result, $y_1^\mu(t)$ is shown in the top left plot with the solid line. The convolution of the functions, $y_1(t)$, is shown in the top right hand plot. The bottom plots illustrates the convolution of $x_2(t) = \cos(8\pi t)\Pi_{100}(t)$ with $h_2(t) = \Pi_{10}(t)$. Note that $x_2(t) = x_1(t)/\mu(t)$ and $h_2(t) = h_1(t)/\mu(t)$. The bottom left plot shows $x_2^\mu(t)$ with a dashed line, $h_2^\mu(t)$ with a dotted line, and $y_2^\mu(t)$ with a solid line. The bottom right plot is the of the same convolution, except $x_2(t)$, $h_2(t)$ and $y_2(t)$ are plotted in lieu of $x_2^\mu(t)$, $h_2^\mu(t)$ and $y_2^\mu(t)$. Note that $y_2(t) \neq y_1(t)/\mu(t)$.

or, using the notation in (6.2),

$$y^\mu(t) = x^\mu(t) \overset{\mathbb{L}_1}{*} h^\mu(t). \tag{6.4}$$

For the following examples, we use \log_{10} for \mathbb{L}_1 .

Examples of the time scale convolution in (6.4) are shown in Figs. 9 and 10. The top row in Fig. 9 shows convolution corresponding to $x_1^\mu(t) = \cos(8\pi t)\Pi_{100}(t)$ with $h_1^\mu(t) = \Pi_{10}(t)$ on \mathbb{L}_1 . The result is $y_1^\mu(t)$. The bottom row shows $y_2(t)$, the convolution when $x_2(t) = \cos(8\pi t)\Pi_{100}(t)$ and $h_2(t) = \Pi_{10}(t)$

The top row in Fig. 10 is convolution corresponding to $x_1^\mu(t) = h_1^\mu(t) = \Pi_6(t)$ on \mathbb{L}_1 . The result is $y_1^\mu(t)$. The bottom row shows $y_2(t)$, the convolution when $x_2(t) = h_2(t) = \Pi_6(t)$.

6.2. Transforms on a random variable

The time scale \mathbb{L}_1 can be used in evaluating the probability mass function of the product of two statistical independent discrete random variables. Let X and H be independent discrete random variables of the lattice type [13]. Let all of the probability mass lie on integers on $\{1, 2, \dots\}$. Let $Y = XH$ so that $\log Y = \log X + \log H$. If the probability mass function for X is p_n at $n = \{1, 2, 3, \dots\}$, then the corresponding probability mass function for the random variable X is

$$p_X(t) = \sum_{n=1}^{\infty} p_n \delta[t - n].$$

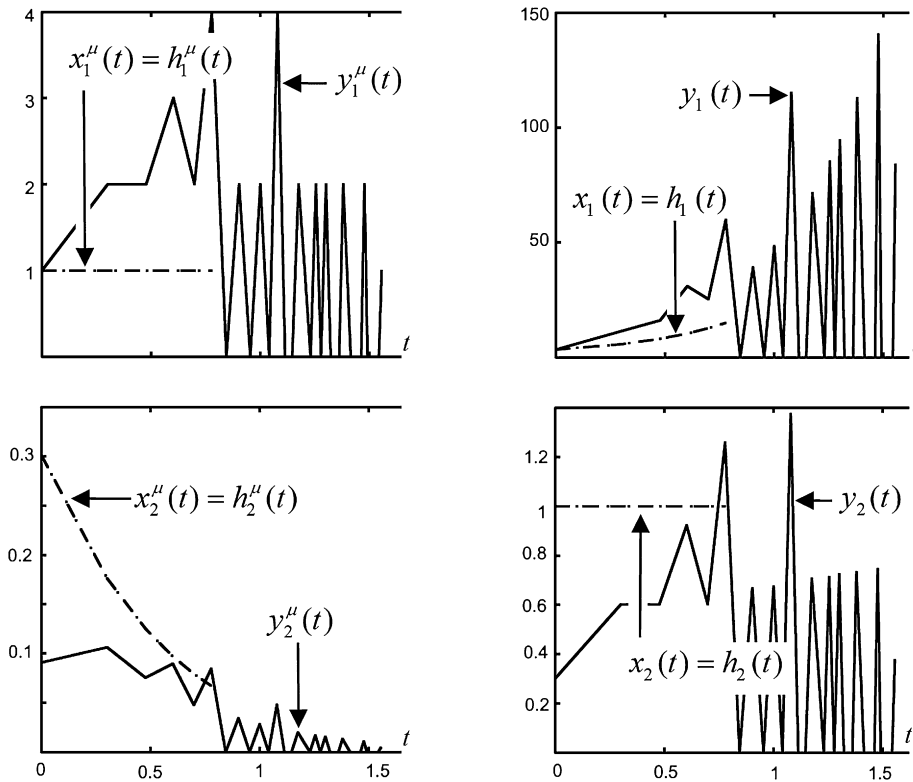


Fig. 10. The top left plot illustrates the \mathbb{L}_1 time scale convolution of $x_1^\mu(t) = \Pi_6(t)$ with $h_1^\mu(t) = x_1^\mu(t)$ shown with the broken line. The result of the time scale convolution, $y_1^\mu(t)$, is plotted with a solid line. It is also plotted in Fig. 11. The top plots are of $x_1(t) = x_1^\mu(t)/\mu(t)$, $h_1(t) = x_1(t)$ and $y_1(t) = y_1^\mu(t)/\mu(t)$. The two bottom plots are of $x_2(t) = \Pi_6(t)$, $h_2(t) = x_2(t)$ and their time scale convolution, $y_2(t)$. Note that $x_2(t) = x_1(t)/\mu(t)$ and $h_2(t) = h_1(t)/\mu(t)$. The result of the convolution is $y_2(t) \neq y_1(t)/\mu(t)$. The bottom plots are the component functions with the subscripts and the right without.

The probability mass function for $\log X$ is then

$$x^\mu(t) = \sum_{n=1}^{\infty} x_n^\mu \delta[t - \log n], \quad x_n^\mu = p_n.$$

The probability mass function, $h^\mu(t)$ on \mathbb{L}_1 , is similarly defined. Since $\log X$ is independent of $\log H$, the probability mass function, $y^\mu(t)$, of their sum, $\log Y$, is given by the time scale convolution on \mathbb{L}_1 of $x^\mu(t)$ with $h^\mu(t)$:

$$y^\mu(t) = x^\mu(t) \overset{\mathbb{L}_1}{*} h^\mu(t) = \sum_{n=1}^{\infty} y_n^\mu \delta[t - \log n], \quad \text{where } y_n^\mu = \sum_{p/n \in \mathbb{N}} x_n^\mu h_{p/n}^\mu. \tag{6.5}$$

The probability mass function for Y is then

$$p_Y(t) = \sum_{n=1}^{\infty} y_n^\mu \delta[t - n]. \tag{6.6}$$

Example 6.1. Two fair die are rolled. The random variable assigned to a showing of n dots on a die is $\log(n)$. The probability mass function for one die is one sixth for points $1 \leq n \leq 6$ on the AITS corresponding to $\log_{10}(n)$. Thus, $x^\mu(t) = h^\mu(t) = \frac{1}{6} \Pi_6(t)$. The sum of the logs of the two dice, $y^\mu(t)$, is given by the time scale convolution of $x^\mu(t)$ and $h^\mu(t)$ and is shown in the top left corner in Fig. 10. The corresponding probability mass function, $p_Y(t)$, is shown in Fig. 11. The mass at $n = 12$ has four realizations, $\{(3, 4), (4, 3), (2, 6), (6, 2)\}$, and therefore has four times the mass at $n = 25$ which only has one realization: $\{(5, 5)\}$.

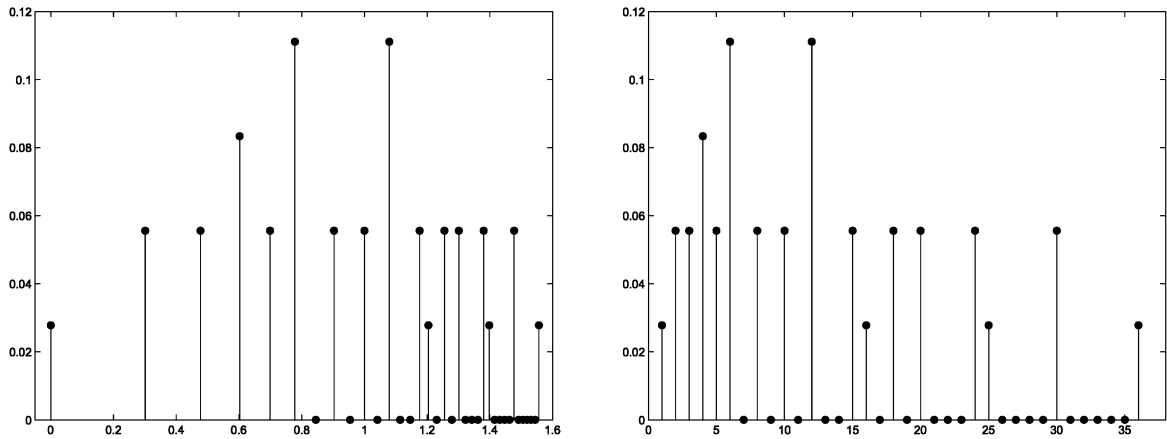


Fig. 11. (Left) An \mathbb{L}_1 time scale convolution result, $y^\mu(t)$, in (6.5) using $x^\mu(t) = h^\mu(t) = \frac{1}{6}\Pi_6(t)$. (Right) The probability mass function, $p_Y(t)$, in (6.6) corresponding to the time scale convolution illustrated in (a). The probability mass is the product of the values showing on the two dice.

6.3. Mellin convolution

The Mellin convolution of discrete sequences $x[n]$ and $h[n]$ is defined by

$$y[n] := \sum_{(k \in \mathbb{N}) \cap (\frac{n}{k} \in \mathbb{N})} x[k]h\left[\frac{n}{k}\right].$$

For the discrete Mellin transform [12],

$$Y_M(\omega) = \sum_{n=1}^{\infty} y[n]n^\omega,$$

it is straightforward to show that

$$Y_M(\omega) = X_M(-\omega)H_M(\omega).$$

Mellin convolution is performed when using the AITS \mathbb{L}_1 . Since $t_p = \log(p)$, the discrete time convolution in (6.1) becomes

$$\begin{aligned} y^\mu(\log(p)) &= \sum_{(\log(p) - \log(n) \in \mathbb{L}_1) \cap (\log(n) \in \mathbb{L}_1)} x^\mu(\log(n))h^\mu(\log(p) - \log(n)) \\ &= \sum_{(\frac{p}{n} \in \mathbb{N}) \cap (n \in \mathbb{N})} x^\mu(\log(n))h^\mu\left(\log\left(\frac{p}{n}\right)\right). \end{aligned}$$

This is a Mellin convolution for $y[p] = y^\mu(t_p)$, $x[n] = x^\mu(t_n)$, and $h[m] = h^\mu(m)$ where $t_q = \tau_q = \xi_q = \log(q)$.

7. Conclusions

In this paper, we developed several tools from Fourier analysis tools in the context of time scales: a generalized Fourier transform, and inversion result, and a convolution for signals on two (possibly distinct) time scales. This brand of convolution leads to several natural classes of time scales which arise in this setting: dilated, closed under addition, and additively idempotent. Finally, we explore a range of problems that can be approached advantageously from this vantage point, e.g. discrete convolution and transformations of a random variable.

References

[1] R. Agarwal, M. Bohner, D. O'Regan, A. Peterson, Dynamic equations on time scales: A survey, J. Comput. Appl. Math. 141 (2002) 1–26.

- [2] M. Bohner, A. Peterson, *Advances in Dynamic Equations on Time Scales*, Birkhäuser, 2003.
- [3] M. Bohner, A. Peterson, *Dynamic Equations on Time Scales: An Introduction with Applications*, Birkhäuser, 2001.
- [4] J.M. Davis, I.A. Gravagne, B.J. Jackson, R.J. Marks II, A.A. Ramos, The Laplace transform on time scales revisited, *J. Math. Anal. Appl.* 332 (2007) 1291–1307.
- [5] R.M. Haralick, *Mathematical Morphology: Theory and Hardware*, Oxford University Press, 2005.
- [6] R.M. Haralick, L.G. Shapiro, *Computer and Robot Vision*, Addison-Wesley, 1991.
- [7] S. Hilger, Analysis on measure chains—A unified approach to continuous and discrete calculus, *Results Math.* 18 (1990) 18–56.
- [8] S. Hilger, An application of calculus on measure chains to Fourier theory and Heisenberg’s uncertainty principle, *J. Difference Equ. Appl.* 8 (2002) 897–936.
- [9] S. Hilger, *Ein Masskettenkalkül mit Anwendung auf Zentrumsmannigfaltigkeiten*, PhD thesis, Universität Würzburg, 1988.
- [10] S. Hilger, Special functions, Laplace and Fourier transform on measure chains, *Dynam. Systems Appl.* 8 (1999) 471–488.
- [11] R.J. Marks II, *Introduction to Shannon Sampling and Interpolation Theory*, Springer-Verlag, 1991.
- [12] R.J. Marks II, J.N. Larson, One-dimensional Mellin transformation using a single optical element, *Appl. Optics* 18 (1979) 754–755.
- [13] A. Papoulis, S.U. Pillai, *Probability, Random Variables and Stochastic Processes*, fourth ed., McGraw–Hill Science, 2001.
- [14] M.A. Soderstrand, *Residue Number System Arithmetic: Modern Applications in Digital Signal Processing*, IEEE Press, 1986.